Origin and Scaling of the Permanent Dipole Moment in CdSe Nanorods

Liang-shi Li and A. Paul Alivisatos*

Department of Chemistry, University of California, Berkeley, California 94720
Materials Sciences Division, Lawrence Berkeley National Laboratory, Berkeley, California 94720
(Received 23 September 2002; published 6 March 2003)

Transient electric birefringence measurements were performed on dilute solutions of CdSe nanorods. The results confirm the existence of a permanent dipole along the *c*-crystallographic axis. Measurements on nanorods with different widths and lengths show that the longitudinal permanent dipole moment scales linearly with volume, suggesting it arise from the noncentrosymmetric crystallographic lattice.

Detailed theoretical and experimental studies of electronic and optical properties of spherical colloidal CdSe nanocrystals with the wurzite structure have greatly improved our understanding of the quantum effects caused by the confinement of electrons and holes in a finite volume [1]. Compared to other types of quantum dots such as III-V dots grown by molecular beam epitaxy [2,3], II-VI colloidal dots have a lower-symmetry hexagonal crystal structure with no inversion center. A longstanding question concerns the possible presence and origin of a ground state dipole moment in these nanocrystals, with rather contradictory prior experimental and theoretical studies [4–8]. A significant permanent ground state dipole moment can alter the electronic level structure, radiative rates, and other fundamental optical properties of the quantum dots. The advent of new synthetic procedures for making extended nanorods of CdSe [9] with controlled aspect ratio [10] affords the opportunity to conclusively determine the presence and scaling of the CdSe dipole moment as a function of length and diameter.

These measurements are of importance not only for our fundamental understanding of quantum confinement in this prototypical quantum dot system, but also as essential background knowledge for the spatial manipulation of nanorods. It has been shown that, when dispersed at high density in a solvent, CdSe nanorods spontaneously form liquid crystalline phases [11]. It is of great interest to use external electric and magnetic fields to align these liquid crystalline samples in order to achieve the manipulation of their orientations on a large scale. As a first step in this direction, however, it is important to have a good understanding of the mechanism of alignment of the noninteracting nanorods in dilute solutions under an externally applied electric field, e.g., alignment as a result of permanent electric dipole moments or anisotropic electric polarizabilities.

Here we use the transient electric birefringence method to study the response of CdSe nanorods with variable widths and lengths under an electric field. Transient electric birefringence (TEB) is a standard method that has been widely used to study the rotational diffusion, size,

shape, and polarization properties of objects with anisotropic geometry, especially macromolecules [12] and biological systems such as DNA, viruses, and proteins [13]. The transient behavior of the birefringence reflects the alignment mechanism of these molecules in response to a pulsed electric field. In particular, for a suspension of elongated objects with axial symmetry and a large aspect ratio (≥ 5), the rising (Δn_r) and falling (Δn_f) edges of the birefringence (difference between the refractive indices of the sample along and perpendicular to the applied electric field) upon application and removal of an external electric field are given, respectively, by [14]

$$\Delta n_r(t) = \Delta n_s \left(1 + \frac{\gamma - 2}{2(\gamma + 1)} \exp(-6D_R t) - \frac{3\gamma}{2(\gamma + 1)} \exp(-2D_R t) \right) \quad \text{and}$$

$$\Delta n_f(t) = \Delta n_s \exp(-6D_R t), \tag{1}$$

where $\Delta n_s = \Delta n_r(t \to \infty)$, $\gamma = \mu_z'^2 / [k_b T(\alpha_\parallel - \alpha_\perp)]$, μ_z' is the screened value [15] of the electric dipole moment along the long axis of the rods, $\alpha_\parallel$ and $\alpha_\perp$ are the static electric polarizability along and perpendicular to the long axis, respectively, and D_R is the rotational diffusion constant around an axis normal to the long axis of the rods. According to Eq. (1), the birefringence rises slower than it falls only when there is a permanent dipole moment along the long axes of the rods. Benoit [14] used this method to study tobacco mosaic virus (TMV), and from the symmetric falling and rising edges he concluded that TMVs do not have permanent dipole moment in aqueous solution.

To measure the electric birefringence, we use the procedure of O'Konski [16,17]. A pulsed electric field is applied transversely to a cell containing the sample between two crossed Glan-Thompson polarizers oriented at 45° to the field. A $\lambda/4$ plate is interposed between the sample and the analyzer. During the measurement, the analyzer is rotated by ~ 1–$4°$ from the crossed position to improve the signal to noise ratio. This angle is much larger than the phase difference between the components of the light polarized along and perpendicular to the

external field within the range of field strength applied, so that the modulation in the transmitted intensity is linear to the phase difference, and therefore to the electrically induced birefringence. The sample cell consists of two 25.0 mm $\times$ 10.0 mm heavily gold-coated copper electrodes that are 1.2 mm apart in a standard 1.0 cm light path glass spectrometer cell, with CdSe nanorod solution in between. The cell is kept at $25.0 \pm 0.1\,°C$ during the measurement. The external voltage is a single-polarity square wave applied by a pulse generator, which allows us to apply a voltage with a rise and fall time shorter than 25 ns. A He-Ne laser (632.8 nm) is used as the light source. The transmitted light is detected with a photomultiplier tube with ~ 10 ns time response, and the transient signal recorded with a 500 MHz digital oscilloscope. The incident beam is attenuated to be in the linear range of the detector. The time response of the whole setup was tested to be smaller than 50 ns by measuring the transient birefringence of nitrobenzene.

The samples we measured are CdSe nanorods with various widths and lengths dispersed in cyclohexane, as shown in Table I. The nanorods have excellent size monodispersity ($\sim 5\%$ for width and 15% for length), as measured from transmission electron micrograph images (TEM). These nanorods are coated with organic ligands such as trioctylphosphine oxide (TOPO). Because these surface ligands have much smaller volume and lower dielectric constants compared to the nanocrystals, their contribution to the electric birefringence is negligible (at least 3 orders of magnitude smaller), as proven by the blank experiments. The solutions of CdSe nanorods we measured were maintained dilute (number density $\ll 1/\text{length}^3$) to avoid interrod coupling. The charging of the CdSe nanocrystals is not significant because no accumulation of nanorods at either of the electrodes was observed when a static voltage was applied for hours.

Figure 1 shows the static birefringence of transmitted light vs electric field. Within the range of the field strength we applied, only linear behavior is observed [18]. These nanorods under electric field have birefringence of the same sign as nitrobenzene, indicating that the nanorods align along (rather than perpendicular to) the electric
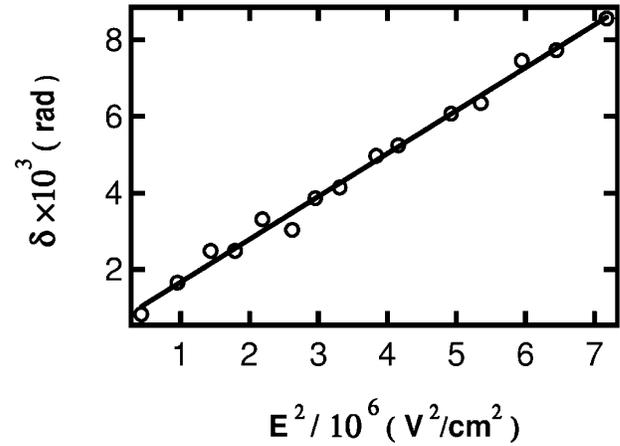

FIG. 1. The static electric birefringence (linear to the phase difference between the two components of the light with polarization along and perpendicular to the applied field). It is linearly proportional to the transmitted intensity under the field with various strengths when the analyzer is rotated by $\sim 4°$ from the cross position. The sample is a dilute solution of 4.8×30 nm CdSe nanorods in cyclohexane.

field. Figure 2(a) shows a typical transient electric birefringence curve measured for CdSe nanorods. As suggested by Eqs. (1), the asymmetric falling and rising edges indicate the existence of a permanent electric dipole moment along the long axis. The hexagonal symmetry of CdSe nanorods allows us to approximately treat them as being axially symmetric, thus we can fit the TEB curves [e.g., Figs. 2(b) and 2(c)] with Eqs. (1) to obtain the rotational diffusion constants and the ratio of permanent dipole moment to the polarizability anisotropy (γ), as listed in Table I.

From the rotational diffusion constants D_R obtained by fitting the TEB curves, we can get the length of the nanorods l with the equation [19]

$$D_R = \frac{3k_bT}{\pi\eta l^3}\left(\ln\frac{2l}{d} - 0.8\right), \qquad (2)$$

where d is the width of the nanorods, as determined from TEM images, and η the viscosity of the solution

TABLE I.

Width[a] (nm)	Length[a] (nm)	Length[b] (nm)	Volume (nm³)	$(6D_R)^{-1}$ (μs)	$\frac{3\gamma}{\gamma-2}$	γ	$\frac{\alpha_\parallel}{4\pi\varepsilon_0}$ (nm³)	$\frac{\alpha_\perp}{4\pi\varepsilon_0}$ (nm³)	μ_z (debye)
3.1 ± 0.1	58 ± 6	60 ± 0.3	302 ± 24	3.61 ± 0.05	5.43 ± 0.38	4.47 ± 0.38	94.4 ± 12.5	31.1 ± 4.1	153.4 ± 23.9
4.8 ± 0.2	26 ± 4	30 ± 0.5	361 ± 29	0.81 ± 0.04	4.24 ± 0.12	6.84 ± 0.46	99.9 ± 14.0	38.1 ± 5.3	209.9 ± 32.6
3.8 ± 0.2	20 ± 3	23 ± 1.6	174 ± 18	0.39 ± 0.08	4.82 ± 0.87	5.30 ± 1.15	47.7 ± 8.2	18.3 ± 3.1	126.4 ± 36.9
3.0 ± 0.1	51 ± 6	54 ± 0.6	254 ± 20	2.83 ± 0.10	6.77 ± 0.82	3.59 ± 0.34	79.2 ± 11.5	26.2 ± 3.8	126.3 ± 21.4
3.0 ± 0.1	33 ± 4	35 ± 1.1	165 ± 14	0.93 ± 0.09	8.17 ± 2.81	3.16 ± 0.64	49.8 ± 8.2	17.1 ± 2.8	95.7 ± 24.6

[a]Measured from TEM images.
[b]Calculated with Eq. (2) from D_R obtained from the electric birefringence measurement. 1.1 nm is subtracted as the solvation shell due to the capping ligands, e.g., TOPO.
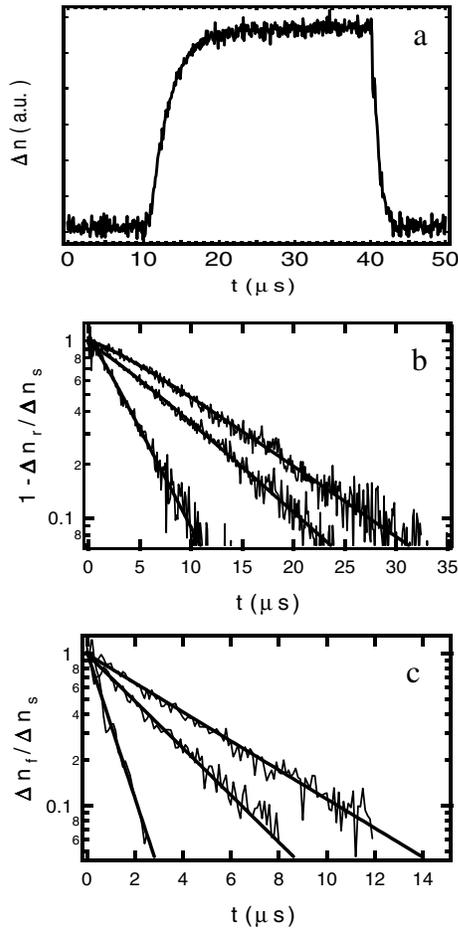
FIG. 2. (a) A typical TEB curve (in linear scale) upon the application and subsequent removal of the electric field. The CdSe nanorods are 4.8 nm wide and 30 nm long. (b),(c) The logarithm scale plots of the fit for the rising and falling edges in the form of Eqs. (1) for the TEB curves of three CdSe nanorod samples. Δn_s is the saturation value of $\Delta n(t)$. In both (b) and (c) from left to right, the CdSe nanorods are 3.0×35, 3.0×54, and 3.1×60 nm (in width and length), respectively.

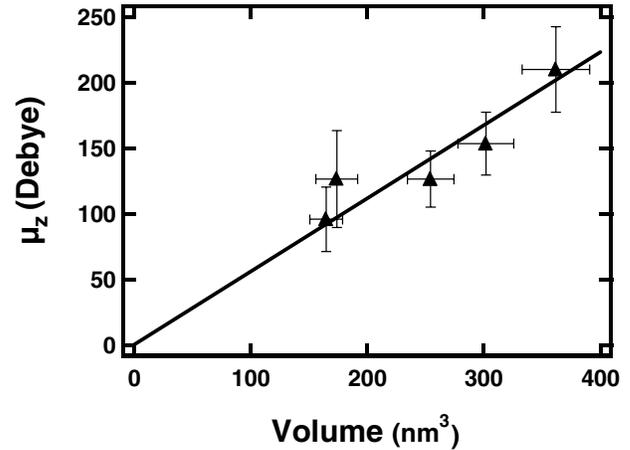

FIG. 3. The unscreened dipole moment of CdSe nanocrystals. The solid triangles are the values measured with the TEB method (Table I), and the straight line the best fit with a slope of 0.19 μC/cm^2.

(0.98 mPa s for cyclohexane at 25 °C). The calculated lengths agree very well (within 10%) with the results from TEM images, confirming that the TEB signals we obtained are due to the CdSe nanorods.

In order to get the permanent dipole moment from γ, we calculate the electric polarizability of CdSe nanorods by assuming a revolute prolate shape, so that the principal axes of polarizability coincide with the geometrical axes. The polarizabilities shown in Table I are calculated with [20]

$$\alpha_{\parallel(\perp)} = \varepsilon_0 v(\varepsilon_{\parallel(\perp)} - 1)/[1 + A_{\parallel(\perp)}(\varepsilon_{\parallel(\perp)} - 1)], \quad (3)$$

where v is the volume of the individual nanorod, ε is the relative dielectric constants between nanorods and the solvent along ($\parallel$) or perpendicular ($\perp$) to the long axis of the nanorods, and A is the geometrical factors deter- mined by the dimension of the nanorods [21]. The dielec- tric constants of CdSe nanorods are taken as bulk material values ($\varepsilon_{\parallel} = 10.2$, $\varepsilon_{\perp} = 9.33$), and that of cyclo- hexane as 2.02.

The unscreened permanent dipole moments μ_z of five nanorod samples (Table I) are plotted in Fig. 3 vs their volume. Considering the ensemble nature of the measure- ment, these are the root mean square dipole moment of the samples over both the finite size distribution and the possible structural distribution [4]. Within the experimen- tal error, however, a linear dependence of μ_z vs volume is obtained, and no correlation between rod length or width and μ_z is observed. This is consistent with theoretical analyses that the polarity is intrinsic to the crystallo- graphic lattice of CdSe [4–7] due to the lack of inversion symmetry, but not with the trapped surface charge model proposed for spherical CdSe nanocrystals [8]. From the slope, we get the polarization of CdSe nanorods to be 0.19 μC/cm^2 along the c-crystallographic axis, in good agreement with the value of 0.6 μC/cm^2, as estimated [7] from a phenomenological rule that was proven experi- mentally only for ferroelectric materials.

It is well known that migrating charges may contribute to the electric dipole moment measured by the TEB method [22,23]. The hopping of trapped charges between different trapping sites on the CdSe nanocrystal surfaces could result in a nonvanishing mean square average di- pole moment even with a vanishing mean dipole moment. This effect can be modeled with a time-dependent elec- tric polarizability. It has been shown [22] that, if the induced dipole due to the migrating charges is predomi- nant over that caused by the lattice and we assume a single exponential form for the polarizability, i.e., $\alpha_{\parallel} - \alpha_{\perp} = q_l + q_c[1 - \exp(-t/\tau)]$, where q_l and q_c are the anisotropy of the polarizability contributed by the lattice and the migrating surface charges, respectively, the rising

edge of the TEB curve would be expressed as [23]

$$\Delta n_r(t) = \Delta n_s\{1 - \exp(-6D_R t) - \exp(-t/\tau) + \exp[-(1/\tau + 6D_R)t]\},$$

where τ is related to the diffusion constant of the surface charges on the surface and scales linearly with the surface area of the nanorods. This is not consistent with our experimental results, which indicate that the contribution of migrating charges on the surfaces of the nanorods is not significant.

The large permanent electric dipole moment along the long axes of the nanorods has important consequences on the thermodynamic stability of liquid crystalline phases of CdSe nanorods. For example, numerical simulation on hard spherocylinders with central longitudinal dipoles [24] showed the destabilization of the nematic phase with respect to the isotropic phase and the stabilization of a smectic-A phase. Further, the large permanent electric dipole moment of the ground state should influence the spatial distribution of optically generated electron-hole pairs, with consequences for both linear and non-linear optical properties of the nanorods.

---

*To whom correspondence should be addressed.
Email address: alivis@uclink4.berkeley.edu

[1] Al. L. Efros and M. Rosen, Annu. Rev. Mater. Sci. **30**, 475 (2000).

[2] R. Leon, P. M. Petroff, D. Leonard, and S. Fafard, Science **267**, 1966 (1995).

[3] J. Heydenreich et al., Phys. Rev. Lett. **74**, 4043 (1995).

[4] E. Rabani, B. Hetényi, B. J. Berne, and L. E. Brus, J. Chem. Phys. **110**, 5355 (1999).

[5] N. Q. Huong and J. L. Birman, J. Chem. Phys. **108**, 1769 (1998).

[6] S. A. Blanton, R. L. Leheny, M. A. Hines, and P. Guyot-Sionnest, Phys. Rev. Lett. **79**, 865 (1997).

[7] M. E. Shmidt, S. A. Blanton, M. A. Hines, and P. Guyot-Sionnest, J. Chem. Phys. **106**, 5254 (1997).

[8] M. Shim and P. Guyot-Sionnest, J. Chem. Phys. **111**, 6955 (1999).

[9] X. Peng et al., Nature (London) **404**, 59 (2000).

[10] L.-S. Li, J. Hu, W. Yang, and A. P. Alivisatos, Nano Lett. **1**, 349 (2001).

[11] L.-S. Li, J. Walda, L. Manna, and A. P. Alivisatos, Nano Lett. **2**, 557 (2002).

[12] C. T. O'Konski, in Encyclopedia of Polymer Science and Technology (Interscience, New York, 1968), Vol. 9, p. 551.

[13] K. Yoshioka and H. Watanabe, in Physical Principles and Techniques of Protein Chemistry, edited by S. J. Leach (Academic, New York, 1969), Pt. A, p. 335.

[14] H. Benoit, Annales de Physique (Paris) **6**, 561 (1951).

[15] The unscreened value can be calculated by multiplying the screened value by the factor $1 + (\varepsilon_\parallel - 1)A_\parallel$, where $\varepsilon_\parallel$ and $A_\parallel$ are defined in Eq. (3).

[16] C. T. O'Konski and B. H. Zimm, Science **111**, 113 (1950).

[17] J. Newman and H. L. Swinney, Biopolymers **15**, 301 (1976).

[18] C. T. O'Konski, K. Yoshioka, and W. H. Orttung, J. Phys. Chem. **63**, 1558 (1959).

[19] J. M. Burgers, Verhandel. Koninkl. Ned. Akad. Wetenschap. Afdeel. Natuurk. **16**, 113 (1938).

[20] C. J. F. Böttcher, Theory of Electric Polarization (Elsevier, New York, 1973).

[21] J. A. Osborn, Phys. Rev. **67**, 351 (1945).

[22] J. G. Kirkwood and J. B. Shumaker, Proc. Natl. Acad. Sci. U.S.A. **38**, 855 (1952).

[23] I. Tinoco, J. Am. Chem. Soc. **77**, 4486 (1955).

[24] S. C. McGrother, A. Gil-Villegas, and G. Jackson, Mol. Phys. **95**, 657 (1998).